

## ARTICLE

# First Principles Study of Electronic Structure and Half-metallicity of Molecule-based Ferromagnet $\text{Cr}[\text{N}(\text{CN})_2]_2$

Hai-ming Huang<sup>a\*</sup>, Shi-jun Luo<sup>a</sup>, Guo-ying Liu<sup>a</sup>, Kai-lun Yao<sup>b,c</sup>

a. School of Science, Hubei University of Automotive Technology, Shiyan 442002, China

b. School of Physics, Huazhong University of Science and Technology, Wuhan 430074, China

c. International Center of Materials Physics, Chinese Academy of Sciences, Shenyang 110015, China

(Dated: Received on December 15, 2010; Accepted on February 14, 2011)

The electronic structure and half-metallicity of molecule-based ferromagnet  $\text{Cr}[\text{N}(\text{CN})_2]_2$  have been investigated using first-principles with generalized gradient approximation. The total energy, spin-polarized electronic band structure, density of states (DOSs) and spin magnetic moments were all calculated. The calculations reveal that the compound  $\text{Cr}[\text{N}(\text{CN})_2]_2$  is a really half-metallic ferromagnet with a integral magnetic moment of  $2.0000 \mu_B$  per molecule in the optimized lattice constant. Based on the spin distribution and the DOS, it is found that the total magnetic moment is mainly from the  $\text{Cr}^{2+}$  with relative small contribution from C and N atoms. The sensitivity of the half-metallicity to small change in lattice constant is also discussed.

**Key words:** First principles, Magnetic property, Half-metallic property

## I. INTRODUCTION

New spintronic devices based on the spin rather than charge played an important role for their promising applications in the future high performance information technologies [1]. Highly spin-polarized ferromagnets, especially half-metallic ferromagnets are key ingredients for the applications of spintronic devices [2]. In 1983, de Groot *et al.* first predicted the half-metallic in  $\text{NiMnSb}$  and  $\text{PtMnSb}$  [3], since then, more half-metallic ferromagnets have been predicted theoretically and confirmed experimentally. Thus far, half-metallic ferromagnets have been found in many types of materials such as transition-metal oxides [4], Heusler alloys [5], dilute magnetic semiconductors [6], and so on. With the rapid development of information technologies, the quest to develop new half-metallic ferromagnets is a growing area of contemporary materials chemistry research. In our study, we have found the half-metallic ferromagnetic (FM) properties exist in purely organic radical crystal [7]. The pure organic magnetic materials have free radicals, which can supply the magnetic moment, but their transition temperatures are too low for practical applications. Many researchers turn their sights to the molecular-based ferromagnet with metallic ions [8–10]. When the metal atoms or metal salt are added in organic materials, they will greatly influence the properties of organic materials. It is necessary to

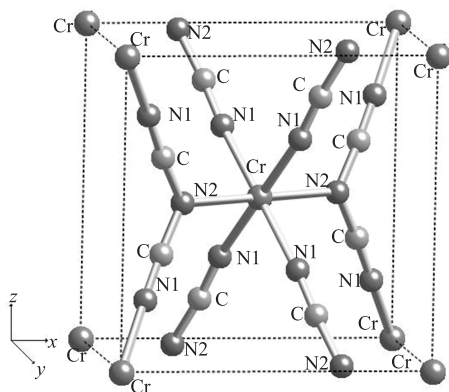
study their electronic structure in order to understand the nature of these materials. This will provides new insights to the origin of the strong ferromagnetic coupling in this family of compounds.

The new family of isostructural compounds with the general formula  $\text{M}[\text{N}(\text{CN})_2]_2$  exhibits particularly interesting magnetic properties. The compounds are composed of transition metal ions ( $\text{M}=\text{Mn}, \text{Fe}, \text{Co}, \text{Ni},$  and  $\text{Cr}$ ) and organic dicyanamide  $[\text{N}(\text{CN})_2]_2$  ligands [11, 12]. They crystallize in a distorted rutile-type 3D structure in which the connectivity between the metals is joined through  $(\text{N}\equiv\text{C}-\text{N}-\text{C}\equiv\text{N})^-$  and  $\text{N}-\text{C}-\text{N}$  linkages. The crystal structures and the magnetic properties have attracted much attention in both theory and experiment as molecular-based magnetic crystals [13–17], whereas, there is no reports on the half-metallicity of these compounds. In this work, we adopt the first principles method to study the electronic structure of the  $\text{Cr}[\text{N}(\text{CN})_2]_2$  and discuss the half-metallicity, which is useful for designing of novel half-metallic ferromagnetic materials.

## II. COMPUTATIONAL DETAILS

The first principles calculation about the real materials based on the density functional theory (DFT) is one of the most powerful tools to calculate the electronic structure of materials. It can give us the information about spin distributions in magnetic materials which are not measured from experiment. Full-potential linearized augmented plane-wave (FP-LAPW) method is one of the most accurate methods for performing elec-

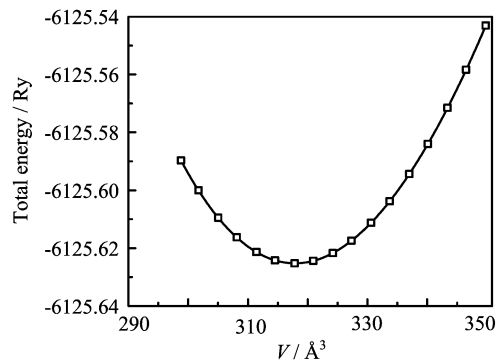
\* Author to whom correspondence should be addressed. E-mail: smilehmm@163.com

FIG. 1 Crystal structure of  $\text{Cr}[\text{N}(\text{CN})_2]_2$ .

electronic structure calculation for crystals. The calculations have been done with Wien2k code [18], the generalized gradient approximation (GGA) [19] is taken for the exchange correlation potential. The GGA is a widely used approximation for the exchange-correlation functional in DFT, proven to be very successful in predicting many material properties [20–22]. The crystal structure of  $\text{Cr}[\text{N}(\text{CN})_2]_2$  was plotted in Fig.1, it crystallizes in the space group  $Pnmm$  ( $Z=2$ ), and the lattice parameters  $a=5.922(2)$  Å,  $b=7.478(3)$  Å,  $c=7.564(3)$  Å,  $\alpha=\beta=\gamma=90^\circ$  [23]. In the self-consistent calculations, the FP-LAPW basis set consists of the  $3d^54s^1$  states of Cr,  $2s^22p^2$  states of C, and  $2s^22p^3$  states of N. The atomic-sphere radii have been chosen as 2.1, 1.0, and 1.0 a.u. for Cr, C, and N, respectively. The maximum value of angular momentum is taken for the wave function expansion inside the atomic spheres. In order to accomplish the energy eigenvalue convergence, the wave function in the interstitial region is expanded in terms of plane waves with a cutoff parameter  $R_{\text{mt}}K_{\text{max}}=5.0$ , where  $K_{\text{max}}$  is the maximum value of the reciprocal lattice vector used in the plane wave expansion, and  $R_{\text{mt}}$  is the smallest atomic-sphere radius of all the atomic spheres. We used  $3 \times 10^3$   $k$ -points in the irreducible wedge of the Brillouin zones for the calculations, and the self-consistent calculations are considered to converge only when the calculated total energy of the crystal converges to less than  $10^{-4}$  Ry.

### III. RESULTS AND DISCUSSION

Before studying electronic structure and magnetic properties, we first fully optimize the volume and atomic positions of  $\text{Cr}[\text{N}(\text{CN})_2]_2$ . Figure 2 presents the calculated total energy versus unit-cell volume of  $\text{Cr}[\text{N}(\text{CN})_2]_2$  and the optimized lattice constant is  $a=5.818(3)$  Å,  $b=7.346(2)$  Å,  $c=7.431(3)$  Å,  $\alpha=\beta=\gamma=90^\circ$ . It can be seen that there is only a slight deviation from the experimental values, which shows that our theoretical calculation is credible.

FIG. 2 The calculated total energy versus volume of  $\text{Cr}[\text{N}(\text{CN})_2]_2$ .

In order to investigate the relative stability of ferromagnetic states with respect to the antiferromagnetic (AFM) ones, we construct  $1 \times 1 \times 2$ ,  $1 \times 2 \times 1$ , and  $2 \times 1 \times 1$  supercells, which contain two primary cells. In the AFM configuration, we suppose the corresponding atoms in the supercell have the same spin magnetic moments orientation. For AFM configuration, we let those atoms in the supercell have opposite spin magnetic moments orientation, respectively. The results show that  $1 \times 1 \times 2$  supercell has the lowest energy both in FM and AFM state. Relative stability of FM structure is indicated by the total energy difference between AFM structure and the FM one in  $1 \times 1 \times 2$  supercell as follows:

$$\Delta E = E_{\text{AFM}} - E_{\text{FM}} \quad (1)$$

where  $E_{\text{FM}}$  and  $E_{\text{AFM}}$  are the total energies of the FM structure and AFM structure. If  $\Delta E$  is positive, the FM phase is stable and if  $\Delta E$  is negative, then AFM state is more stable. The results reveal that the total energy difference  $\Delta E$  is about 0.011 Ry, the FM state has the lowest energy among the two configurations. So the FM phase is a stable ground state and the AFM phase is a metastable state for  $\text{Cr}[\text{N}(\text{CN})_2]_2$ , which is in good agreement with the experimental results.

Figure 3 presents the spin-dependent band structure of  $\text{Cr}[\text{N}(\text{CN})_2]_2$ . The spin splitting can be clearly seen between the majority-spin and minority-spin states near the Fermi level. The band structure of the majority-spin bands keeps semiconductor behavior with the band gap 1.21 eV, while the minority-spin channel saddles the Fermi level and shows the metallic properties. The feature of the band structure of the ferromagnetic ground state of  $\text{Cr}[\text{N}(\text{CN})_2]_2$  shows half-metallic behavior with a half-metallic band gap of 0.19 eV. Half-metallic gap is an important parameter to determine the application in spintronic devices, which is defined as the minimum of  $E_c$  and  $E_v$ , where  $E_c$  is the energy value of the bottom of majority-spin conduction band with respect to the Fermi level and  $E_v$  is the absolute value of the energy from the top of majority-spin valence band to the Fermi level. If  $\text{Cr}[\text{N}(\text{CN})_2]_2$  is really a half-metallic ferromagnet, it may be important to spin electronics.

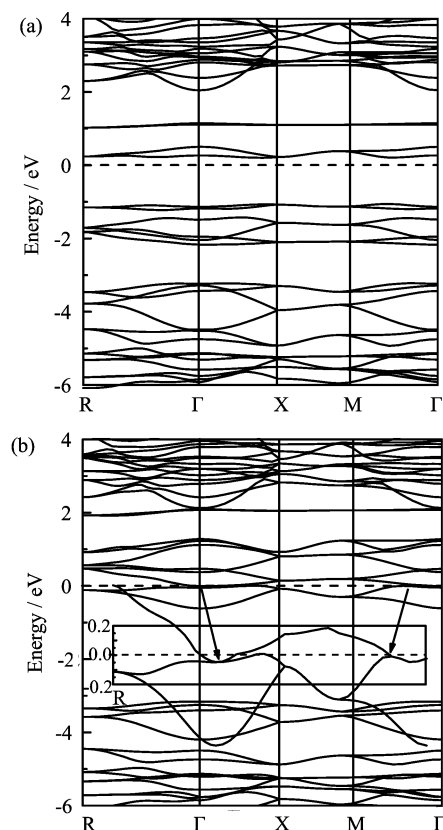


FIG. 3 The spin-dependent band structure of  $\text{Cr}[\text{N}(\text{CN})_2]_2$ . (a) Majority-spin, (b) minority-spin. The Fermi level is indicated by the dashed horizontal line.

The spin-dependent total and local density of states (DOSs) of  $\text{Cr}[\text{N}(\text{CN})_2]_2$  are presented in Fig.4(a) and Fig.5. The plotted energy range is from  $-6$  eV to  $4$  eV. Because only the DOS distribution near the Fermi level determines the electric conductivity, we concentrate our attention upon the DOS in the vicinity of the Fermi level. The spin populations on chromium, cobalt, and nitrogen are dominated by  $3d$  or  $2p$  states, respectively. An asymmetrical distribution of the DOS can be seen between the majority-spin and minority-spin states around the Fermi level, especially, the minority-spin states crossing the Fermi level are partially filled, whereas the majority-spin states have a large band gap at the Fermi energy in the bands of the majority-spin electrons, which confirms the half-metallicity of  $\text{Cr}[\text{N}(\text{CN})_2]_2$  once again. Comparing Fig.4(a) with Fig.5, we can see that the  $2p$  states of C, N1, and N2 occupy the lowest part of the valence band and upper part of the conductor band, the occupied states near the Fermi level are mainly from  $3d$  states of Cr, with relative small contribution from  $2p$  states of C, N1, and N2.

Careful investigating the DOS distribution near the Fermi level in Fig.5, we can find that hybridization exist between  $\text{Cr}3d$ ,  $\text{N}2p$  and  $\text{C}2p$  states near the Fermi

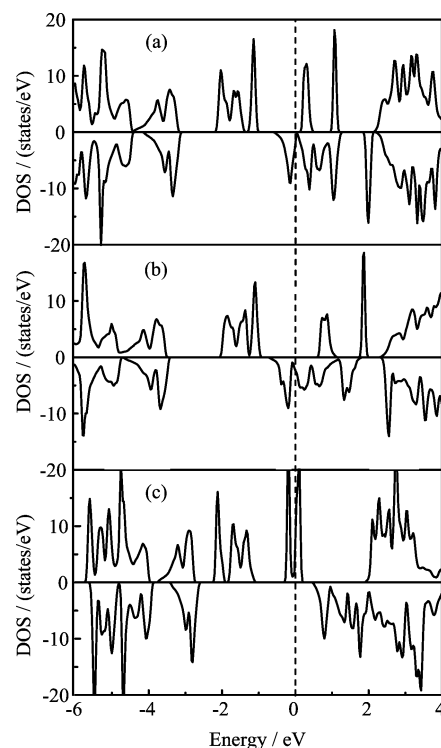


FIG. 4 The total density of state for  $\text{Cr}[\text{N}(\text{CN})_2]_2$  in different structures. (a) Optimized structure, (b) the lattice constant is compressed 5%, (c) the lattice constant is extended 5%. In each panel, the positive and negative values correspond to the majority-spin and minority-spin states. The  $x$ -axis zero level corresponds to the Fermi level.

level. The DOS profiles of the  $\text{Cr}3d$  and neighboring N1  $2p$  states near the Fermi level are very similar, they occupy the same range and vary with the same shape, just with different magnitudes. One can also find that the partial DOS of the  $\text{C}2p$  and neighboring N2  $2p$  states are similar to a certain extend near the Fermi level. Whereas, the hybridization between the former is stronger than that between the latter, which demonstrates that the origin of magnetic properties of  $\text{Cr}[\text{N}(\text{CN})_2]_2$ . The asymmetrical distributions of the DOS and hybridization mean the magnetism of molecule-based ferromagnet. We conclude the magnetic property is mainly originated from the Cr atoms because they play an important role around the Fermi level. The total magnetic moment of  $\text{Cr}[\text{N}(\text{CN})_2]_2$  and spin magnetic moments of different atoms are shown in Table I.

Spin-polarization calculations show the total magnetic moment is  $2.0000 \mu_B$  per molecule. The integral value is typical character of half-metallic ferromagnets. We can find that the major part of the magnetic moment is mainly from  $\text{Cr}^{2+}$ , and C and N make a relatively small contribution, indicating that the  $\text{Cr}^{2+}$  lies in the high-spin state, which is in very good agreement with the density of states. The negative sign in the

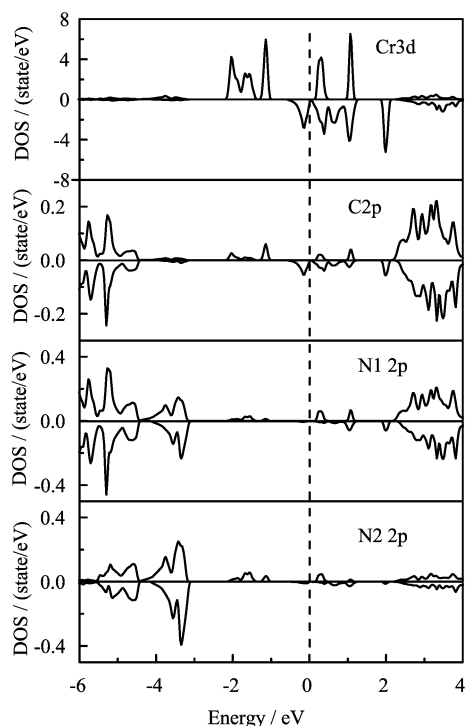


FIG. 5 The partial density of states for  $\text{Cr}[\text{C}(\text{CN})_3]_2$ . The positive and negative values correspond to the majority-spin and minority-spin states. The  $x$ -axis zero level corresponds to the Fermi level.

TABLE I The total magnetic moment of  $\text{Cr}[\text{N}(\text{CN})_2]_2$  and spin magnetic moments of different atoms in  $\mu_B$ .

Structure	Cr	C	N1	N2	Total
Optimized	1.8145	0.0011	-0.0068	0.0003	2.0000
5% compressed	1.7357	0.0012	-0.0034	0.0007	2.0000
5% extended	3.3823	0.0152	-0.0062	0.0009	4.0000

spin magnetic moments of the N1 demonstrates that the N1 atom is antiparallel to that of neighboring Cr and C atoms. We note that the spin magnetic moment of  $\text{Cr}^{2+}$  is only  $1.8145 \mu_B$ , which is smaller than the free space charge value  $4.0000 \mu_B$ . Due to this strongly antiferromagnetic coupling and the spin frustration, the local magnetic moment of  $\text{Cr}^{2+}$  reduces from its free space charge value and produces the small spin magnetic moments on the C, N1, and N2 atoms.

On the other hand, in order to investigate the sensitivity of the half-metallicity to small change in lattice constant, we performed the spin-polarized calculation on  $\text{Cr}[\text{N}(\text{CN})_2]_2$  when the lattice constant of which is compressed and extended 5%. The corresponding DOSs are plotted in Fig.4 (b) and (c). We notice that the majority-spin states obviously are away from the Fermi level and the majority-spin states slightly move towards the Fermi level in the vicinity of Fermi level when the lattice constant is compressed. The opposite phenomena can be observed when the lattice constants is ex-

tended. Much to our surprise, the majority-spin states cut the Fermi level and shows the metallic properties, while the minority-spin states keep the semiconductor character, which is different from the optimized structure. Even then, the half-metallicity of  $\text{Cr}[\text{N}(\text{CN})_2]_2$  is maintained in those structures. Table I also presents the total magnetic moments and atomic spin magnetic moments when the lattice constant is changed. For the extended structure, the  $\text{Cr}^{2+}$  has the magnetic moment  $3.3823 \mu_B$ , which is close to the free space charge value  $4.0000 \mu_B$ . It indicates the valence electronic spin alignment of  $\text{Cr}^{2+}$  in  $\text{Cr}[\text{N}(\text{CN})_2]_2$  is affected by the lattice constant, and we expect the experimental confirmation in the future.

#### IV. CONCLUSION

We have studied the electronic structure, half-metallicity and magnetic properties of  $\text{Cr}[\text{N}(\text{CN})_2]_2$  by first-principles with GGA. The results show that the compound has stable ferromagnetic ground state, which is in good agreement with the experimental results. The analysis of the spin distribution and the DOS demonstrate that the spin magnetic moment is mainly from the  $\text{Cr}^{2+}$  with relative small contribution from C, N1, and N2 atoms. Moreover, the sensitivity of the half-metallicity to a small change in lattice constant is discussed, which indicates that the spin alignment of valence electron may be changed in  $\text{Cr}^{2+}$  when the lattice constant is extended. All the results show the  $\text{Cr}[\text{N}(\text{CN})_2]_2$  is a really half-metallic ferromagnet, which is promising for spintronic devices or designing of novel half-metallic ferromagnetic materials.

#### V. ACKNOWLEDGMENTS

This work was supported by the the National Natural Science Foundation of China (No.10974048) and the Excellent Middle Age and Youth People Science and Technology Creative Team Foundation of the Educational Department of the Hubei Province (No.T200805).

- [1] S. A. Wolf, D. D. Awschalom, R. A. Buhrman, J. M. Daughton, S. Von Molnar, M. L. Roukes, A. Y. Chtchelkanova, and D. M. Treger, *Science* **294**, 1488 (2001).
- [2] Y. H. Zhao, G. P. Zhao, Y. Liu, and B. G. Liu, *Phys. Rev. B* **80**, 224417 (2009).
- [3] R. A. de Groot, F. M. Müeller, P. G. van Engen, and K. H. J. Buschow, *Phys. Rev. Lett.* **50**, 2024 (1983).
- [4] V. Srivastava, M. Rajagopalan, and S. P. Sanyal, *Eur. Phys. J. B* **61**, 131 (2008).
- [5] G. Gökoğlu and O. Gülseren, *Eur. Phys. J. B* **76**, 321 (2010).

- [6] H. Pan, Y. P. Feng, Q. Y. Wu, Z. G. Huang, and J. Y. Lin, *Phys. Rev. B* **77**, 125211 (2008).
- [7] S. J. Luo and K. L. Yao, *Phys. Rev. B* **67**, 214429 (2003).
- [8] H. M. Huang, S. J. Luo, and K. L. Yao, *J. Magn. Magn. Mater.* **321**, 2200 (2009).
- [9] K. L. Yao, L. Zhu, and Z. L. Liu, *Eur. Phys. J. B* **39**, 283 (2004).
- [10] L. Y. Zhu and J. L. Wang, *J. Phys. Chem. C* **113**, 8767 (2009).
- [11] H. Köehler, A. Kolbe, and G. Lux, *Z. Anorg. Allg. Chem.* **428**, 103 (1977).
- [12] M. Kurmoo and C. J. Kepert, *New J. Chem.* **22**, 1515 (1998).
- [13] L. Zhu, K. L. Yao, and Z. L. Liu, *Chem. Phys. Lett.* **424**, 209 (2006).
- [14] A. Lappas, A. S. Wills, M. A. Green, M. Kurmoo, and K. Prassides, *Phys. Rev. B* **67**, 144406 (2003).
- [15] F. X. Zu and S. Z. Xia, *Phys. Lett. A* **349**, 384 (2006).
- [16] A. S. Wills and A. Lappas, *J. Phys. Chem. Solids* **65**, 65 (2004).
- [17] M. R. Pederson, A. Y. Liu, T. Baruah, E. Z. Kurmaev, A. Moewes, S. Chiuzbăian, M. Neumann, C. R. Kmety, K. L. Stevenson, and D. Ederer, *Phys. Rev. B* **66**, 014446 (2002).
- [18] P. Blaha, K. Schwarz, G. K. H. Madsen, D. Kvasnicka, and J. Luitz, *WIEN2k, An Augmented-Plane-Wave+Local Orbitals Program for Calculating Crystal Properties*, Austria: Karlheinz Schwarz, (2001).
- [19] J. P. Perdew, K. Burke, and M. Ernzerhof, *Phys. Rev. Lett.* **77**, 3865 (1996).
- [20] J. Liu, P. D. Chen, L. Chen, H. N. Dong, and R. L. Zheng, *Chin. J. Chem. Phys.* **23**, 397 (2010).
- [21] C. W. Zhang and S. S. Yan, *J. Appl. Phys.* **107**, 043913 (2010).
- [22] Y. T. Yang, F. G. Wu, and Z. G. Wei, *Chin. J. Chem. Phys.* **22**, 497 (2009).
- [23] J. L. Manson, C. R. Kmety, A. J. Epstein, and J. S. Miller, *Inorg. Chem.* **38**, 2552 (1999).